



Supplement of

Technical note: Interpreting pH changes

Andrea J. Fassbender et al.

Correspondence to: Andrea J. Fassbender (andrea.j.fassbender@noaa.gov)

The copyright of individual parts of the supplement might differ from the CC BY 4.0 License.

S1. Determination of 2010 mean pH values

Mean pH values provided in the supplemental information of Munro et al., (2015) were adjusted to the year 2010 using the pH trends and observing periods reported in Munro et al., (2015). The mean $[H^+]$ value for Station ALOHA provided in the main text of Dore et al. (2014) was adjusted to the year 2010 using the $[H^+]$ trend and observing period 5 reported in Dore et al. (2014) and converted to pH. Mean pH values were calculated for all other locations using (a) 12-month pH climatology data constructed from available time-series site data and referenced to the year 2010 or (b) a 2010-normalized, global $3^\circ \times 3^\circ$ gridded pH climatology based on Version 4 of the Surface Ocean CO₂ Atlas (SOCAT-v4; Bakker et al., 2016), as described in Fassbender et al. (2017). The 2010 mean pH values are listed in Table S1. The 2010 mean $[H^+]$ values described in Text S2 were computed from 2010 mean pH values. All pH (and 10 $[H^+]$) values are given at in situ temperatures.

S2. Calculation of pH and $[H^+]$ trends and their uncertainties

pH trends and uncertainties (u) are provided in the main text of Bates et al. (2014; defined as one standard error of the slopes) and Sutton et al. (2014; defined as the measurement uncertainty propagated through a weighted linear 15 regression) as well as in the supplemental information of Munro et al. (2015; defined as one standard error of the slopes). The $[H^+]$ trend and uncertainty (defined as one standard error of the slope) for Station ALOHA are provided in the main text of Dore et al. (2014) and were used along with the mean $[H^+]$ value (adjusted to 2010) to compute the pH trend and uncertainty. The two pCO_2 trends and uncertainties given in the main text of Sutton et al. (2019) were converted to $[H^+]$ trends and uncertainties using the local, 2010-referenced, climatological (*clim.*) $d[H^+]/dpCO_2$ 20 sensitivity derived from the SOCAT-v4 gridded data product described in Fassbender et al. (2017). That sensitivity is expected to change only marginally over the 21st century (see Hagens and Middelburg, 2016). At each location considered, the $[H^+]$ trend and its uncertainty are given by:

$$\left(\frac{d[H^+]}{dt} \right) = \left(\frac{d[H^+]}{dpCO_2} \right)_{clim.} \times \left(\frac{dpCO_2}{dt} \right) \quad (1)$$

$$u \left(\frac{d[H^+]}{dt} \right) = \left(\frac{d[H^+]}{dpCO_2} \right)_{clim.} \times u \left(\frac{dpCO_2}{dt} \right) \quad (2)$$

25 pH values were then calculated by applying the $[H^+]$ trend to the 2010 mean value ($\overline{[H^+]}$) in increments of 1 year from $t = 0$ to 9 to simulate one decade.

$$pH(t) = -\log \left(\overline{[H^+]} + (t - 4.5) \times \left(\frac{d[H^+]}{dt} \right) \right) \quad (3)$$

A simple linear regression was then applied to the pH values resulting from Eq. (3) to estimate the 10-year pH trend. To estimate pH trend uncertainty for the two sites from Sutton et al. (2019), the pH trend was divided by the $[H^+]$ 30 trend (to determine the local sensitivity of pH to $[H^+]$ changes) and multiplied by the $[H^+]$ trend uncertainty.

$$u(pH) = u \left(\frac{d[H^+]}{dt} \right) \times \left(\left(\frac{dpH}{dt} \right) \times \left(\frac{d[H^+]}{dt} \right)^{-1} \right) \quad (4)$$

pH trends and uncertainties are presented in Table S1 and Fig. S1.

Table S1. Mooring and ship-based time-series site names, latitudes, longitudes, sea surface pH trends, pH trend uncertainties, pH trend observing periods, and the literature references from which these data were obtained. Also included are estimates of the 2010 mean pH value for each site and the literature references from which these mean values were obtained. All values are at in situ temperature on the total hydrogen ion scale.

Location	Lat. (°N)	Lon. (°E)	pH Trend (yr ⁻¹)	pH Trend Uncertainty (yr ⁻¹)	pH Trend Observing Period	pH Trend Reference	Mean pH in 2010	Mean pH Reference
170 °W	0.00	190.00	-0.0010	0.0004	2005-2011	1	7.996	4a
155 °W	0.00	205.00	-0.0022	0.0003	1998-2011	1	7.998	4a
140 °W	0.00	220.00	-0.0018	0.0004	2004-2011	1	7.981	4a
125 °W	0.00	235.00	-0.0026	0.0005	2004-2011	1	7.973	4a
Iceland	68.00	347.34	-0.0014	0.0005	1983-2009	2	8.110	4b
Irminger	64.30	332.00	-0.0026	0.0006	1983-2005	2	8.081	4b
BATS	32.00	296.00	-0.0017	0.0001	1983-2012	2	8.085	4b
ESTOC	29.04	344.50	-0.0018	0.0002	1995-2012	2	8.074	4a
CARIACO	10.50	295.32	-0.0025	0.0004	1995-2012	2	8.047	4a
Munida	-45.70	171.50	-0.0013	0.0004	1998-2012	2	8.090	4a
DP N (R1)	-57.00	296.00	-0.0019	0.0002	2002-2015	3	8.061	3
DP S (R4)	-61.50	298.00	-0.0015	0.0003	2002-2015	3	8.060	3
WHOTS	22.67	202.02	-0.0019	0.0003	2004-2014	5	8.056	4a
Stratus	-19.70	274.40	-0.0015	0.0003	2006-2015	5	8.062	4a
ALOHA/HOT	22.75	202.00	-0.0017	0.0001	1988-2012	6	8.077	6

¹Sutton et al., 2014

²Bates et al., 2014

³Munro et al., 2015: Mean pH values were adjusted to the year 2010 using the pH trends and observing periods.

⁴Fassbender et al., 2017: 2010 centered (a) SOCAT-v4 global climatology and (b) time-series site climatologies.

⁵Sutton et al., 2019: *p*CO₂ trends and uncertainties were converted to pH trends and uncertainties using the calculations outlined in Text S2 of this study

⁶Dore et al., 2014: pH values were calculated from [H⁺] information provided in the manuscript. The mean [H⁺] value was adjusted to the year 2010 using the [H⁺] trend and observing period.

50

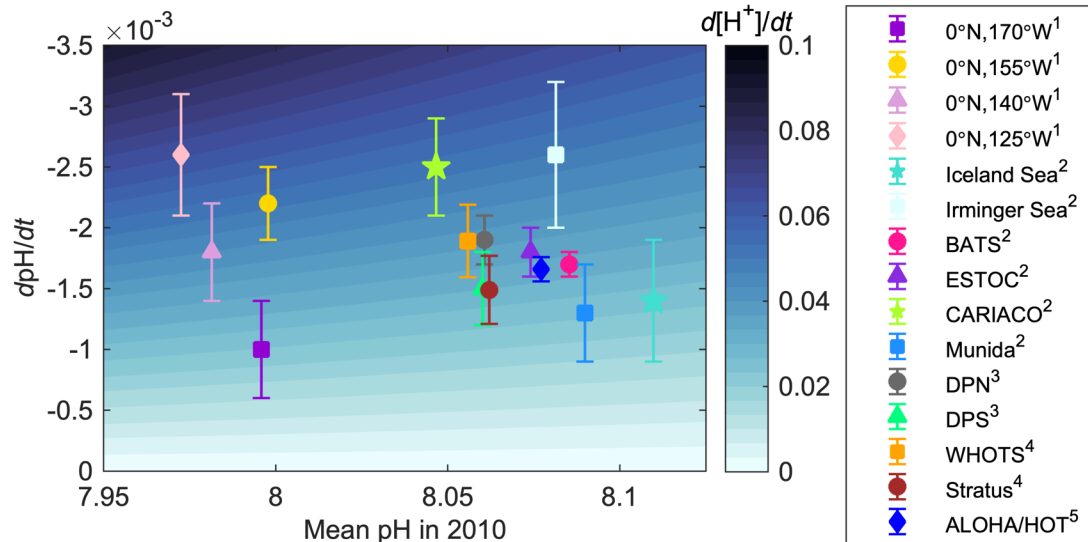
55

Table S2. Mooring and ship-based time-series site names, latitudes, longitudes, and literature references from which these data were obtained. The right six columns show pH and $[H^+]$ values calculated from GFDL ESM2M model output for the combined historical and RCP8.5 experiments for total alkalinity, pCO_2 , silicate, phosphate, salinity, and temperature using the MATLAB program CO2SYS version 1.1 (van Heuven et al., 2011; Lewis and Wallace, 1998). The dissociation constants of *Mehrback et al.* [1973] as refit by *Dickson and Millero* [1987], the hydrogen sulfate dissociation constant of *Dickson et al.* [1990], and the boron-to-chlorinity ratio of *Uppström* [1974] were applied in these calculations, following the approach used for ESM2M. Provided are the average 1950s and 2090s annual mean sea surface pH and $[H^+]$ (nmol kg^{-1}) values and the change in decadal average sea surface pH and $[H^+]$ (nmol kg^{-1}) seasonal cycle amplitude (ΔA) between the 1950s and 2090s. Decadal averages were smoothed with a running mean filter using a four-element, sliding window to reduce the influence of natural variability.

Location	Lat. (°N)	Lon. (°E)	Ref.	1950s Annual Mean pH	2090s Annual Mean pH	2090s- 1950s ΔA -pH	1950s Annual Mean $[H^+]$ (nmol kg^{-1})	2090s Annual Mean $[H^+]$ (nmol kg^{-1})	2090s- 1950s ΔA - $[H^+]$ (nmol kg^{-1})
ALAWAI	21.28	202.15	1	8.154	7.770	-0.013	7.022	16.992	0.5987
BOBOA	14.97	89.93	1	8.122	7.770	0.008	7.562	17.008	1.121
BTM	31.50	295.80	1	8.148	7.783	-0.008	7.129	16.553	1.710
CAPEELIZABETH	47.35	235.27	1	8.285	7.829	-0.083	5.263	14.916	2.185
CCE1	33.50	237.49	1	8.121	7.740	-0.031	7.598	18.243	1.018
CCE2	33.48	239.19	1	8.134	7.756	-0.020	7.384	17.585	1.649
CHABA	47.97	234.63	1	8.214	7.752	-0.066	6.148	17.750	1.048
CHEECAROCKS	24.91	279.38	1	8.127	7.783	-0.008	7.480	16.497	1.251
CHUUK	7.46	151.90	1	8.116	7.761	0.008	7.650	17.335	0.786
COASTALMS	30.00	271.40	1	8.219	7.828	-0.032	6.113	14.972	2.422
CRESCENTREEF	32.40	295.21	1	8.153	7.784	-0.004	7.048	16.479	1.603
CRIMP1	21.43	202.21	1	8.154	7.770	-0.013	7.022	16.992	0.599
CRIMP2	21.46	202.20	1	8.154	7.770	-0.013	7.022	16.992	0.599
GAKOA	59.85	210.50	1	8.189	7.736	-0.059	6.502	18.371	0.383
GRAYSREEF	31.40	279.13	1	8.148	7.792	-0.005	7.138	16.200	1.893
GULFOFMAINE	43.02	289.46	1	8.139	7.774	-0.004	7.275	16.835	1.202
HOGREEF	32.46	295.17	1	8.153	7.784	-0.004	7.048	16.479	1.603
ICELAND	68.00	347.30	1	8.219	7.753	-0.038	6.063	17.751	1.653
JKEO	37.93	146.52	1	8.168	7.783	-0.005	6.797	16.503	1.265
KANEOHE	21.48	202.22	1	8.154	7.770	-0.013	7.022	16.992	0.599
KEO	32.28	144.58	1	8.162	7.772	-0.014	6.915	16.950	1.701
KILONALU	21.29	202.14	1	8.154	7.770	-0.013	7.022	16.992	0.599
KODIAK	57.70	207.69	1	8.154	7.732	-0.011	7.029	18.564	1.091
LAPARGUERA	17.95	292.95	1	8.128	7.778	-0.007	7.447	16.672	0.665
M2	56.51	195.96	1	8.146	7.727	-0.006	7.161	18.782	1.449
NH10	44.90	235.22	1	8.163	7.750	-0.047	6.908	17.795	0.638
PAPA	50.13	215.16	1	8.145	7.732	-0.009	7.179	18.533	1.045
SEAK	56.26	225.33	1	8.219	7.789	0.006	6.046	16.281	1.808
SOFS	-46.80	142.00	1	8.143	7.757	0.008	7.192	17.509	1.167
STRATUS	-19.70	274.40	1	8.133	7.778	-0.010	7.370	16.677	0.523
TAO110W	0.00	250.07	1	8.047	7.739	-0.015	8.984	18.254	0.054
TAO125W	-0.18	235.59	1	8.059	7.746	-0.013	8.738	17.964	-0.015

Location	Lat. (°N)	Lon. (°E)	Ref.	1950s Annual Mean pH	2090s Annual Mean pH	2090s- 1950s ΔA-pH	1950s Annual Mean [H ⁺] (nmol kg ⁻¹)	2090s Annual Mean [H ⁺] (nmol kg ⁻¹)	2090s- 1950s ΔA- [H ⁺] (nmol kg ⁻¹)
TAO140W	0.00	220.13	1	8.069	7.751	-0.013	8.531	17.750	-0.067
TAO155W	0.00	205.00	1	8.079	7.755	-0.016	8.342	17.577	-0.170
TAO165E	0.01	164.97	1	8.097	7.760	-0.011	7.999	17.378	0.050
TAO170W	-0.04	189.95	1	8.087	7.758	-0.015	8.184	17.472	-0.143
TAO8S165E	-8.04	164.79	1	8.115	7.761	0.004	7.674	17.347	0.723
WHOTS	22.67	202.02	1	8.154	7.770	-0.015	7.017	17.004	0.591
BATS	32.00	296.00	2	8.148	7.783	-0.008	7.129	16.553	1.710
HOT	22.75	202.00	2	8.154	7.769	-0.016	7.030	17.028	0.573
Iceland	68.00	347.34	2	8.219	7.753	-0.038	6.063	17.751	1.653
Irminger	64.30	332.00	2	8.173	7.773	-0.028	6.752	16.914	1.505
Munida	-45.70	171.50	2	8.171	7.788	0.008	6.759	16.344	1.809
ESTOC	29.04	344.50	2	8.147	7.788	-0.009	7.137	16.305	0.894
CARIACO	10.50	295.33	2	8.096	7.775	-0.007	8.023	16.783	0.528
DPN	-57.00	296.00	3	8.134	7.747	-0.014	7.341	17.920	0.165
DPS	-61.50	298.00	3	8.162	7.741	-0.023	6.897	18.186	0.230

60

¹Sutton et al., 2019²Bates et al., 2014³Munro et al., 2015

65

Figure S1. Contour plot showing linearized trends in $[H^+]$ ($\text{nmol kg}^{-1} \text{yr}^{-1}$) associated with mean (or initial) pH values referenced to the year 2010 and the corresponding pH trends. The y axis is reversed so that larger magnitude pH trends are near the top left corner. Symbols show observed and calculated surface ocean pH trends and uncertainties (at in situ temperature) at ocean time-series sites, where legend superscripts refer to ¹Sutton et al. (2014), ²Bates et al. (2014), ³Munro et al. (2015), ⁴Sutton et al. (2019), and ⁵Dore et al. (2014). These sites include: four equatorial Pacific locations, Iceland Sea, Irminger Sea, Bermuda Atlantic Time-series Study (BATS), European Station for Time series in the Ocean at the Canary Islands (ESTOC), CArbon Retention In A Colored Ocean sites in the North Atlantic (CARIACO), Munida, two sites in the Drake Passage north (DPN) and south (DPS) of the Antarctic Polar Front, the Woods Hole Oceanographic Institution HOT Station (WHOTS), the Stratus site, and the ALOHA/Hawaii Ocean

70

75

Time-series (HOT) site. The Drake Passage sites equate to Regions 1 (DPN) and 4 (DPS) in Munro et al., (2015). Details regarding the determination of mean pH values referenced to the year 2010 as well as pH trends and uncertainties for these time-series sites are described in Text S1 and Text S2 and presented in Table S1.

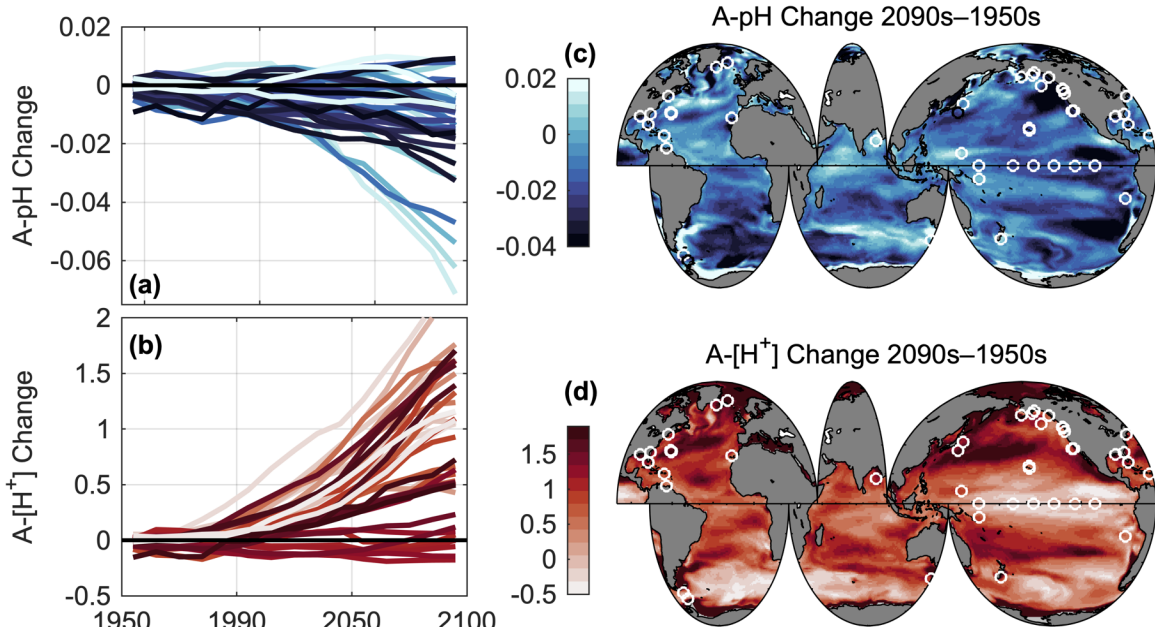


Figure S2. Data used in this figure come from the GFDL ESM2M model for the combined historical and RCP8.5 experiments. Surface ocean seasonal cycle amplitudes (A) were averaged for each decade and smoothed with a running mean filter using a four-element, sliding window. Shown are the decadal changes in (a) A-pH and (b) A-[H⁺] (nmol kg⁻¹) relative to the 1950s at model grids corresponding to time-series site locations in ¹Bates et al. (2014), ²Munro et al. (2015), and ³Sutton et al. (2019; Table S2). Global maps show the total change in (c) A-pH and (d) A-[H⁺] (nmol kg⁻¹) between the 1950s and 2090s. White circles represent the time-series site locations for data presented in a and b. Simulated 1950s and 2090s annual mean pH and [H⁺] values as well as 2090s minus 1950s change in A-pH and A-[H⁺] at each of the 47 locations are listed in Table S2.

References

- Bakker, D. C. E., Pfeil, B., Landa, C. S., Metzl, N., O'Brien, K. M., Olsen, A., Smith, K., Cosca, C., Harasawa, S., Jones, S. D., Nakaoka, S., Nojiri, Y., Schuster, U., Steinhoff, T., Sweeney, C., Takahashi, T., Tilbrook, B., Wada, C., Wanninkhof, R., Alin, S. R., Balestrini, C. F., Barbero, L., Bates, N. R., Bianchi, A. A., Bonou, F., Boutin, J., Bozec, Y., Burger, E. F., Cai, W.-J., Castle, R. D., Chen, L., Chierici, M., Currie, K., Evans, W., Featherstone, C., Feely, R. A., Fransson, A., Goyet, C., Greenwood, N., Gregor, L., Hankin, S., Hardman-Mountford, N. J., Harley, J., Hauck, J., Hoppema, M., Humphreys, M. P., Hunt, C. W., Huss, B., Ibánhez, J. S. P., Johannessen, T., Keeling, R., Kitidis, V., Kötzinger, A., Kozyr, A., Krasakopoulou, E., Kuwata, A., Landschützer, P., Lauvset, S. K., Lefèvre, N., Lo Monaco, C., Manke, A., Mathis, J. T., Merlivat, L., Millero, F. J., Monteiro, P. M. S., Munro, D. R., Murata, A., Newberger, T., Omar, A. M., Ono, T., Paterson, K., Pearce, D., Pierrot, D., Robbins, L. L., Saito, S., Salisbury, J., Schlitzer, R., Schneider, B., Schweitzer, R., Sieger, R., Skjelvan, I., Sullivan, K. F., Sutherland, S. C., Sutton, A. J., Tadokoro, K., Telszewski, M., Tuma, M., van Heuven, S. M. A. C., Vandemark, D., Ward, B., Watson, A. J. and Xu, S.: A multi-decade record of high-quality fCO_2 data in version 3 of the Surface Ocean CO₂ Atlas (SOCAT) Dorothee, Earth Syst. Sci. Data, 8(2), 383–413, doi:10.5194/essd-8-383-2016, 2016.
- Bates, N., Astor, Y., Church, M. J., Currie, K., Dore, J., Gonaález-Dávila, M., Lorenzoni, L., Muller-Karger, F., Olafsson, J. and Santana-Casiano, J. M.: A time-series view of changing ocean chemistry due to ocean uptake of anthropogenic CO₂ and ocean acidification, Oceanography, 27(1), 126–141, doi:10.5670/oceanog.2014.16, 2014.
- Dickson, A. G., Wesolowski, D. J., Palmer, D. A. and Mesmer, R. E.: Dissociation constant of bisulfate ion in aqueous sodium chloride solutions to 250°C, J. Phys. Chem., 94(20), 7978–7985, doi:10.1021/j100383a042, 1990.

- 110 Dickson, A. G. G. and Millero, F. J. J.: A comparison of the equilibrium constants for the dissociation of carbonic acid in seawater media, Deep Sea Res. Part A. Oceanogr. Res. Pap., 34(10), 1733–1743, doi:10.1016/0198-0149(87)90021-5, 1987.
- 115 Dore, J. E., Church, M. J., Karl, D. M., Sadler, D. W. and Letelier, R. M.: Paired windward and leeward biogeochemical time series reveal consistent surface ocean CO₂ trends across the Hawaiian Ridge, Geophys. Res. Lett., 41(18), 6459–6467, doi:10.1002/2014GL060725, 2014.
- Fassbender, A. J., Sabine, C. L. and Palevsky, H. I.: Nonuniform ocean acidification and attenuation of the ocean carbon sink, Geophys. Res. Lett., 44(16), 8404–8413, doi:10.1002/2017GL074389, 2017.
- Hagens, M. and Middelburg, J. J.: Generalised expressions for the response of pH to changes in ocean chemistry, Geochim. Cosmochim. Acta, 187, 334–349, doi:10.1016/j.gca.2016.04.012, 2016.
- 120 van Heuven, S. M. A. C., Pierrot, D., Rae, J. W. B., Lewis, E. and Wallace, D. W. R.: MATLAB program developed for CO₂ system calculations, ORNL/CDIAC-105b. Carbon Dioxide Inf. Anal. Center, Oak Ridge Natl. Lab. U.S. Dep. Energy, Oak Ridge, Tennessee, doi:10.3334/CDIAC/otg.CO2SYS_MATLAB_v1.1, 2011.
- Lewis, E. and Wallace, D. W. R.: Program developed for CO₂ system calculations, Carbon Dioxide Inf. Anal. Center, Oak Ridge Natl. Lab. U.S. Dep. Energy, Oak Ridge, Tennessee. Environ. Sci. Div. Publ. No. 4735 [online] 125 Available from: <https://www.ncdc.noaa.gov/ocads/oceans/CO2SYS/co2rprt.html> (Accessed 2 July 2014), 1998.
- Mehrback, C., Culberson, C. H., Hawley, J. E. and Pytkowicz, R. M.: Measurement of the apparent dissociation constants of carbonic acid in seawater at atmospheric pressure, Limnol. Oceanogr., 18(6), 897–907, doi:10.4319/lo.1973.18.6.0897, 1973.
- 130 Munro, D. R., Lovenduski, N. S., Takahashi, T., Stephens, B. B., Newberger, T. and Sweeney, C.: Recent evidence for a strengthening CO₂ sink in the Southern Ocean from carbonate system measurements in the Drake Passage (2002–2015), Geophys. Res. Lett., 42(18), 7623–7630, doi:10.1002/2015GL065194, 2015.
- Sutton, A. J., Feely, R. A., Sabine, C. L., McPhaden, M. J., Takahashi, T., Chavez, F. P., Friederich, G. E. and Mathis, J. T.: Natural variability and anthropogenic change in equatorial Pacific surface ocean pCO₂ and pH, Global Biogeochem. Cycles, 28(2), 131–145, doi:10.1002/2013GB004679, 2014.
- 135 Sutton, A. J., Feely, R. A., Maenner-Jones, S., Musielwicz, S., Osborne, J., Dietrich, C., Monacci, N., Cross, J., Bott, R., Kozyr, A., Andersson, A. J., Bates, N. R., Cai, W.-J., Cronin, M. F., De Carlo, E. H., Hales, B., Howden, S., D., Lee, C. M., Manzello, D. P., McPhaden, M. J., Meléndez, M., Mickett, J. B., Newton, J. A., Noakes, S. E., Noh, J. H., Olafsdottir, S. R., Salisbury, J. E., Send, U., Trull, T. W., Vandemark, D. C. and Weller, R. A.: Autonomous seawater pCO₂ and pH time series from 40 surface buoys and the emergence of anthropogenic trends, Earth Syst. Sci. Data, 11(1), 421–439, doi:10.5194/essd-11-421-2019, 2019.
- 140 Uppström, L. R.: The boron-chlorinity ratio of deep seawater from the Pacific Ocean, Deep. Res. Part I, 21, 161–162, 1974.